Eur. Phys. J. B **19**, 75–85 (2001)

THE EUROPEAN PHYSICAL JOURNAL B

EDP Sciences

Percolation in two-scale porous media

V.V. Mourzenko[1,3], J.-F. Thovert[1], and P.M. Adler[2,a]

[1] LCD-PTM, SP2MI, BP 179, 86960 Futuroscope Cedex, France
[2] IPGP, tour 24, 4 Place Jussieu, 75252 Paris Cedex 05, France
[3] EPFL, 1015 Lausanne, Switzerland

Received 17 August 2000

Abstract. Two-scale porous media are generated by filtering a Gaussian random correlated field with a random correlated threshold field. The percolation threshold and the critical exponent ν are derived with the help of a finite-size scaling method. The percolation threshold for the three-dimensional media is a decreasing function of the variance and correlation length of the threshold field. A simplified model predicts these trends in 3d; moreover, it suggested some effects in 2d which were all numerically verified.

PACS. 61.43.Gt Powders, porous materials – 61.43.Hv Fractals; macroscopic aggregates (including diffusion-limited aggregates) – 64.60.Ak Renormalization-group, fractal, and percolation studies of phase transitions

1 Introduction

Percolation studies which first analyzed completely disordered discrete systems (*cf.* [1], for a general presentation) are now addressing models with spatial correlations. Various results obtained for short-correlated systems [2,3] and for long-correlated systems [4–6] show that the percolation characteristics of these systems may significantly differ from those of uncorrelated random lattices. This fact is very important because many natural media are not completely random and have spatial correlations in their internal structure.

Porous media consisting of a void phase and a solid phase have a complex morphology, which can be described by a phase function. Theoretical studies of the effective macroscopic properties of porous media are often based on a discrete model with correlated phase function, whose characteristic length is related to mean pore size (see [7–15]). Various methods are used in computer generations of spatially correlated lattices; most of them are based either on thresholding of Gaussian correlated random fields [10,11], or on simulated annealing methods [11]. This list of references is far from being complete, but most of the relevant literature can be obtained from it.

The correlation properties of the porous medium, generated by using a single level cut of a Gaussian field Y, depend on the covariance function of the latter; in the case where it is characterized by a single correlation length, L_Y, the porous medium can be considered as a continuum on scales much larger than L_Y. The porosity, which can be defined as the spatial mean of the phase function, does not vary with distance on these scales and has a single-value parameter characterizing the porous medium.

However, many real porous media are not characterized by a single length scale. Examples include concrete, as shown by Garboczi and Bentz [16], and Vosges sandstones which were analyzed by Adler and Thovert [17]. The quantitative and systematic characterization of such media, which are sometimes called in this paper heterogeneous porous media, has hardly started yet and only a few attempts can be found; the most important is the local porosity theory due to Hilfer [18,19], which generalizes the characterization of the random microgeometry in terms of the average porosity ϵ by local porosity distributions and local percolation probabilities. A complete survey of this topic has recently been done by Hilfer [20].

Let us now turn to the generation of media with multiple scales. Firstly, an interesting process due to Fernandes *et al.* [21], is based on the multiscale percolation systems which were introduced by Neimark [22]. Another possible way is to use invasion percolation (*cf.* [23]); a porous medium is initially filled with a fluid and then invaded by a second fluid, each resulting phase can be considered as a particular pore space.

Hazlett [24] suggested that global spatial correlation statistics, such as in the classical reconstruction technique, should be supplemented with local variability and connectivity informations.

Simultaneously, processes inspired by the threshold of Gaussian fields are appearing now in the literature. The basic idea is to generate two independent fields. In one-scale process, the field $Y(\mathbf{x})$ is thresholded by a constant threshold related to the porosity ϵ. The generalization of this process consists of the removal of the constancy of ϵ.

[a] e-mail: adler@ipgp.jussieu.fr

Adrover and Giona [25] used a variable, but deterministic cut-off; Berk [26] and subsequently Roberts [27,28] used the intersection set between two 2-cut random fields; it is a variant of this technique which is used in the following.

The major purpose of this paper is to generate and study two-scale materials, such as Vosges sandstones, which can be characterized by a random porosity. In order to describe the structure of such media, a variant of the method based on thresholded Gaussian random fields is used. The threshold is also a random correlated Gaussian field with a correlation length L_ϵ, which is larger than L_Y. This variant is described in Section 2. The medium appears as being composed of patches of high and low porosities which are locally homogeneous. The finite-size scaling method, which is used in percolation analysis, is briefly recalled. Some general characteristics of porosity and covariance are discussed in Appendices A and B. A theoretical argument is proposed in Section 3 to address situations which could not be treated numerically, with large ratios between the scales of the microstructure and of the porosity variations. This argument allows to predict general trends relative to the influence of the second scale on the percolation threshold. It is shown that in particular, different effects can be observed in 2 and 3 dimensions, and that the sign and amplitude of the threshold variations depend on the porosity probability distribution. This is illustrated in 2 dimensions by two examples where the percolation threshold may be changed or not.

The rest of the paper is devoted to three-dimensional porous media because it is directed towards real applications; this induces some drastic restrictions. For instance, if one requires a gain of a factor of 10 in the size of the porous medium, this will necessitate a gain in the memory size by a factor of 1000; not to mention the time constraints. This simple fact limits the range of the parameters studied.

The methodology was first tested with one-scale media, as described in Appendix C. The results for the percolation threshold and critical exponent ν from numerical simulations on two-scale media are presented in Section 4.

A good agreement is observed between the two approaches, theoretical and numerical, when they are both applicable.

2 General

2.1 Formulation of the problem

A porous medium is locally described by the binary three-dimensional random phase function $Z(\mathbf{r})$, defined as follows

$$Z(\mathbf{r}) = \begin{cases} 1, & \text{if } \mathbf{r} \text{ belongs to the pore space} \\ 0, & \text{otherwise.} \end{cases} \quad (1)$$

In order to numerically construct the phase function, a random Gaussian field $Y(\mathbf{r})$ with zero mean and unit standard deviation is generated first. The spatial statistical properties of Y are described by the covariance function

$$C_Y(\mathbf{r},\mathbf{s}) = \langle [Y(\mathbf{r}) - \langle Y\rangle][Y(\mathbf{s}) - \langle Y\rangle]\rangle\,. \quad (2)$$

In this study, an isotropic Gaussian covariance function is used

$$C_Y(r) = \exp\left[-(r\pi/L_Y)^2\right], \quad (3)$$

where $r = \|\mathbf{r}-\mathbf{s}\|$, and L_Y is the correlation distance.

The field Z is extracted from Y by a nonlinear filter

$$Z(\mathbf{r}) = \begin{cases} 1, & p(Y(\mathbf{r})) \geq \epsilon(\mathbf{r}) \\ 0, & p(Y(\mathbf{r})) < \epsilon(\mathbf{r}) \end{cases} \quad (4)$$

$$p(y) = \frac{1}{\sqrt{2\pi}} \int_{-\infty}^{y} \mathrm{e}^{-y^2/2}\mathrm{d}y$$

where $\epsilon(\mathbf{r})$ is the threshold and varies with position.

Thus, the generated porous medium is composed of a set of pores with mean size of order L_Y with a varying porosity $\epsilon(\mathbf{r})$. When $\epsilon(\mathbf{r})$ is a constant, the corresponding medium depends on a single scale and is called a one-scale porous medium; such media have been studied by us extensively in the past. Though $\epsilon(\mathbf{r})$ may be any function, deterministic or not, it is assumed here to be a random normally distributed field with mean E and standard deviation S. In this general study, it is convenient to describe its spatial statistical properties by an isotropic Gaussian covariance function

$$C_\epsilon(r) = S^2 \exp\left[-(r\pi/L_\epsilon)^2\right]. \quad (5)$$

Relation (5) implies that porosity is a variable field for scales smaller than L_ϵ; the corresponding medium is called a two-scale porous medium; the two scales are L_Y and L_ϵ. For scales $r \gg L_\epsilon$ porosity can be again considered as constant. Note that when S is equal to 0, the standard one-scale media studied by Adler [10] are obtained.

The generation procedure is schematically illustrated in Figure 1.

The porosity m of a generated sample of porous medium is defined as

$$m = \overline{Z}, \quad (6)$$

where the overbar denotes the spatial average. This value is also a random variable, and it is different for different realizations of porous media. The statistical mean of m is

$$\langle m\rangle = \langle\overline{Z}\rangle = \langle Z\rangle. \quad (7)$$

It should be noted that the random normally distributed variable ϵ can take nonphysical values $\epsilon < 0$ and $\epsilon > 1$. In these cases, the statistical expectancy of Z is 0 and 1 respectively. Hence, $\langle m\rangle$ is not equal to E; instead, it is a function of E and S. It seems preferable to plot the results as functions of $\langle m\rangle$ rather than E; the relationship between these various quantities is detailed in Appendix A and is represented in Figure 2.

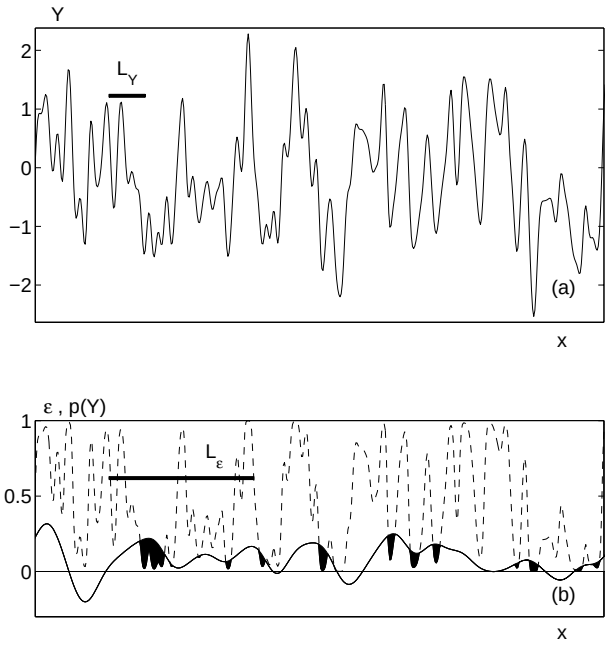

Fig. 1. Schematic view of the generation procedure for a one-dimensional process $Y(x)$ with a correlation length L_Y (a). The random one-dimensional porosity field with a correlation length L_ϵ is displayed in (b) (solid line); it is used to threshold $p(Y)$ (dashed line, see (4)); the black zones in (b) correspond to pores.

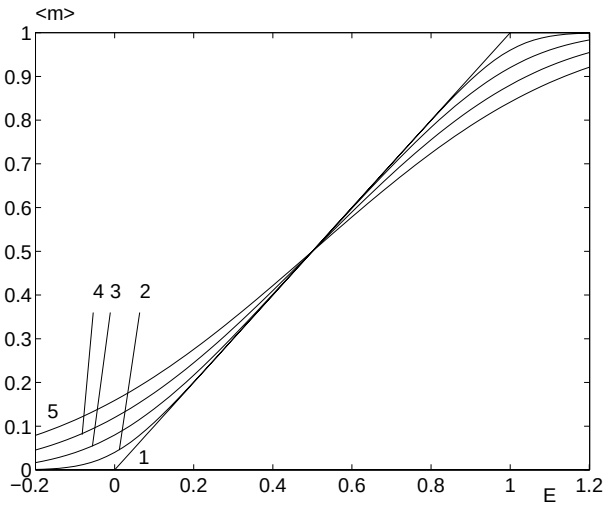

Fig. 2. Mean porosity $\langle m \rangle$ as a function of E for fixed $S = 0$, 0.1, 0.2, 0.3 and 0.4 (1–5).

The spatial statistical properties of the phase function $Z(\mathbf{r})$ are described by the covariance function

$$C_Z(\mathbf{r}, \mathbf{s}) = \langle [Z(\mathbf{r}) - \langle Z \rangle][Z(\mathbf{s}) - \langle Z \rangle] \rangle. \tag{8}$$

This covariance function is studied in Appendix B; its variations are illustrated in Figure 3.

Since it is impossible to generate fields of an arbitrarily large extent, the porous medium is replaced by a three-dimensional spatially periodic medium, which is

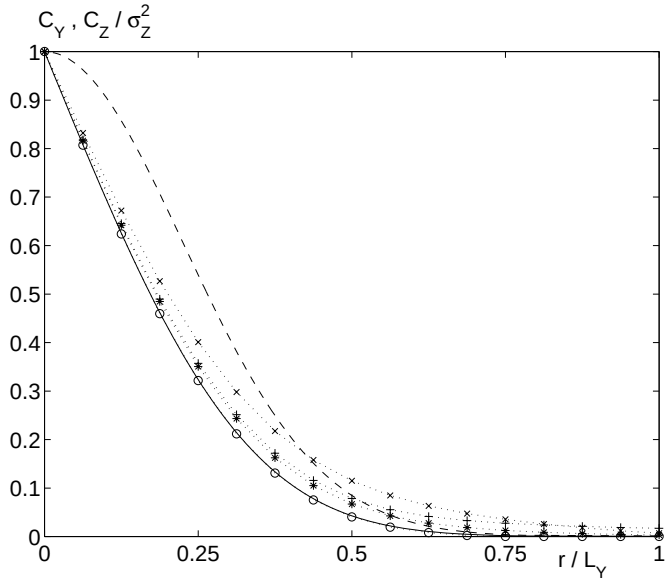

Fig. 3. The covariance C_Y (− − −−) and the normalized covariance C_Z/σ_Z^2 as functions of the distance r/L_Y. Numerical data are obtained from one realization of a porous medium with $L = 200a$, $L_Y = 16a$, $m = 0.201$. C_Z/σ_Z^2 is given for an one-scale medium ($S = 0$, ———), and for two-scale media with $L_\epsilon = L_Y$, $S = 0.1$, $E = 0.2$ (○); $L_\epsilon = 2L_Y$, $S = 0.1$, $E = 0.2$ (⋆); $L_\epsilon = 2L_Y$, $S = 0.2$, $E = 0.181$ (×); $L_\epsilon = 3L_Y$, $S = 0.1$, $E = 0.2$ (+).

composed of identical unit cells of size L. Correlated random Gaussian fields are generated by the method of Fourier transforms on a regular cubic grid with spacings $\Delta x = \Delta y = \Delta z = a$ (see [10,29] for details). This corresponds to the projection of the off-lattice medium (4) onto the a-lattice; in order that no spurious discretization effect occurs, a should be much smaller than L_Y.

Figure 4 shows examples of generated porous media. The influence of the second length scale is clearly visible in Figures 4b and c.

In order to analyze the percolating probability of porous media, N realizations of samples with given a, L_Y, L_ϵ, L, E and S were generated. In agreement with standard practice (*cf.* [1]), the percolation probability P was defined as the fraction of realizations that contain a percolation cluster. As in a classical study of site percolation, each node is supposed to be connected with its first nearest neighbors in the x-, y-, and z-directions, but not with its second nearest neighbors. First, connected components are determined; second, nonpercolating clusters are eliminated by means of a pseudodiffusion process (see [30], for details).

A realization is said to percolate when it percolates along a given direction (this corresponds to the rule R_1 as defined by Reynolds *et al.* [31]); recall that the porous media are spatially periodic along the x-, y- and z-directions; thus, a cluster is percolating along the x-direction if two homologous points in cells with different x-coordinates can be connected through the cluster. Moreover, for each realization, tests in x-, y- and z-directions were considered

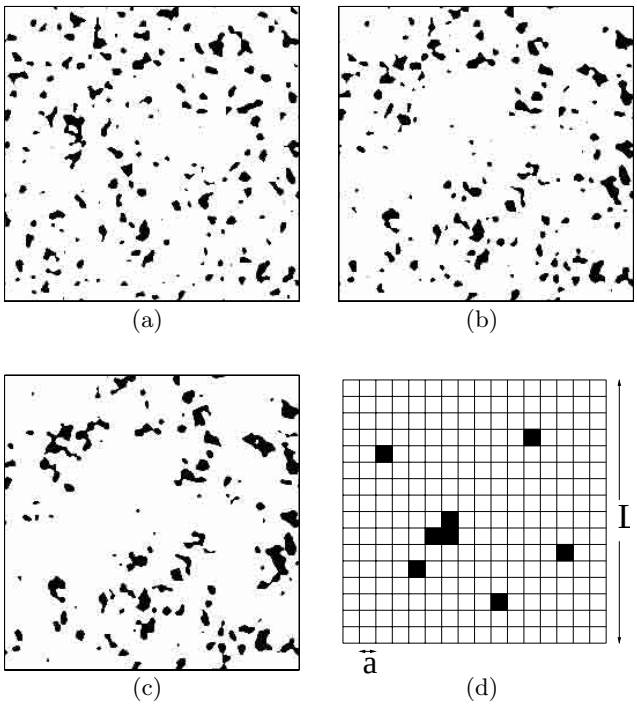

Fig. 4. Examples of generated porous media. Data are for $\langle m\rangle = 0.1$, $L_\epsilon/L_Y = 3$; S is equal to 0 (a), 0.1 (b) and 0.2 (c); corresponding values of E are 0.1, 0.09 and 0.038, respectively. Black zones correspond to pores. The regular grid with spacing a is made visible in (d) for a small value of $L = 16$.

as independent ones; thus, as an example, P is equal to 2/3 for a medium which percolates along x and y only.

The two characteristic lengths L_Y and L_ϵ, and the two artificial lengths a and L, which are necessarily introduced in any numerical scheme, may be ordered as

$$a < L_Y \leq L_\epsilon < L/2. \tag{9}$$

The latter inequality is dictated by the necessity for the sample size to be larger than twice the correlation length L_ϵ; this is because of the overall periodic conditions.

Generally speaking, dimensionless quantities only depend on $\langle m\rangle$ (or equivalently E), S and on the ratios of the lengths which appear in (9)

$$F\left(\langle m\rangle, S, \frac{L_Y}{L_\epsilon}, \frac{a}{L_Y}, \frac{L_\epsilon}{L}\right). \tag{10}$$

Examples of such dimensionless quantities F could be provided by macroscopic properties such as the percolation threshold, the conductivity and the permeability.

Among these five parameters, only the three first ones correspond to real physical quantities. The parameters a/L_Y and L_ϵ/L are artificial in the sense that they are introduced by the discretization scale a and by the size L of the unit cell.

Meaningful results correspond to the limits $a/L_Y \to 0$, $L_\epsilon/L \to 0$. For instance, the percolation threshold m_c is obtained by the standard finite-size scaling method [1] and by an adequate extrapolation of $a/L_Y = 0$. This important point will be detailed in Section 2.2.

2.2 Finite-size scaling method

The finite-size scaling method is often used in percolation analysis and is only briefly recalled here. First, for each set of parameters a, L_Y, L_ϵ and S, the percolation probability $P(\langle m\rangle)$ is tentatively fitted by a two-parameter error function

$$P = \frac{1}{\sqrt{2\pi}\Delta_a}\int_{-\infty}^{\langle m\rangle} \exp\left[-\frac{(\xi - m_a)^2}{2\Delta_a^2}\right] \mathrm{d}\xi, \tag{11}$$

where m_a is the average concentration and Δ_a is the width of the transition region [1]. These parameters depend on the last four parameters in (10). First, extrapolated values m_a^* and Δ_a^* must be determined in the limit $a/L_Y \to 0$

$$m_a^* = \lim_{a/L_Y\to 0} m_a \quad \Delta_a^* = \lim_{a/L_Y\to 0} \Delta_a. \tag{12}$$

Once m_a^* and Δ_a^* are found, the percolation threshold m_c is defined as the limit of m_a^* when $L_\epsilon/L \to 0$, *i.e.*, when the sample size tends to infinity

$$m_\mathrm{c} = \lim_{L_\epsilon/L\to 0} m_a^* = \lim_{L_\epsilon/L\to 0}\left(\lim_{a/L_Y\to 0} m_a\right). \tag{13}$$

The critical exponent ν and m_c can be derived from the scaling laws [1]

$$m_a^* - m_\mathrm{c} \sim \left(\frac{L}{\mathcal{L}}\right)^{-1/\nu}, \tag{14a}$$

$$\Delta_a^* \sim \left(\frac{L}{\mathcal{L}}\right)^{-1/\nu} \tag{14b}$$

where $\mathcal{L}$ is the largest physical scale in the medium. For random uncorrelated, correlated one- and two-scale media, $\mathcal{L}$ is equal to a, L_Y and L_ϵ, respectively.

First, a linear fit of the log-log plot of Δ_a^* *vs.* $L/\mathcal{L}$ is used in order to find ν. Then m_c is estimated from a linear extrapolation of the dependency of m_a^* upon $(L/\mathcal{L})^{-1/\nu}$ in the limit $L = \infty$. Note that even if we are mostly interested in the percolation threshold, it is necessary to derive ν as well.

3 Theoretical approach for large L_ϵ/L_Y

3.1 Very large values of L_ϵ/L_Y

Consider first the extreme case where L_ϵ/L_Y tends to infinity, and S is not vanishingly small. Due to the long range variations of ϵ, regions much larger than L_Y are uniformly above or below $m_\mathrm{c,h}$ which is defined as the percolation threshold for one-scale media (see Appendix C). The pores in a region where ϵ is larger than $m_\mathrm{c,h}$, percolate; such a region is called percolating (denoted by region P). In the opposite case, $\epsilon < m_\mathrm{c,h}$, the pores do not percolate and the corresponding region is called non percolating (denoted by region NP). The distribution of these two

regions has the same spatial correlation as the porosity. Then, global percolation occurs if the volume fraction of region P exceeds the threshold $m_{\mathrm{c,h}}$. Since porosity obeys a Gaussian probability law, this can be expressed as

$$\frac{1}{\sqrt{2\pi}} \int_{\frac{m_{\mathrm{c,h}}-E}{S}}^{+\infty} \mathrm{e}^{-\epsilon^2/2} \mathrm{d}\epsilon = 1 - p\left(\frac{m_{\mathrm{c,h}}-E}{S}\right) \geq m_{\mathrm{c,h}} \tag{15a}$$

or

$$E \geq E_{\mathrm{c}}^{\infty}(S) = m_{\mathrm{c,h}} + \sqrt{2}\, S\, \mathrm{erf}^{-1}\left(2m_{\mathrm{c,h}} - 1\right), \quad (L_\epsilon/L_Y \to \infty). \tag{15b}$$

3.2 Large values of L_ϵ/L_Y

Consider now large but finite ratios L_ϵ/L_Y. Large regions where ϵ is uniformly above or below $m_{\mathrm{c,h}}$ still exist, but they are separated by a transition layer of non vanishing thickness δ, where ϵ is near $m_{\mathrm{c,h}}$ and percolation occurs randomly, according to the probability law (11). The problem of estimating δ has already been addressed in the literature.

Rosso *et al.* [32] studied percolation in site lattices with a site occupancy probability $p(x)$ that monotonically decreases along the x-direction. Thus, the volume fraction of occupied sites ranges from 1 on the left edge to 0 on the right edge of the sample. Similarly, Quintanilla and Torquato [33] studied percolation in two-dimensional continuous heterogeneous media made up of randomly located conducting disks, with a density of disk centers that monotonically increases along the x-direction. The percolating cluster is defined as the set of occupied sites connected to the left edge.

Both models can be viewed as a zoom into the transition layer between low- and high-porosity region in our systems although the microstructure is different. In the model of [33], the disk radius plays the role of the microscale L_Y and the disk volume fraction corresponds to the position dependent field ϵ, whereas the uncorrelated lattices of [32] correspond to $L_Y = 0$.

The percolating cluster frontier is of course an irregular curve or surface, and the range of its excursions from its mean position corresponds to the transition layer. For a linear grade of the disk volume fraction, with constant gradient G, Quintanilla and Torquato [33] showed that the standard deviation σ_x of the frontier excursion in the x-direction is given by

$$\sigma_x \propto R\, \ell^{\frac{\nu}{1+\nu}}, \qquad \ell = \frac{1}{GR}\cdot \tag{16}$$

The same expression applies for the uncorrelated lattices of [32] with R replaced by the lattice unit and G by gradient of site occupancy probability.

In our case, the value of δ can be estimated by equating the width Δ_a of the percolation transition, as given by equation (C.1b) and the typical variation $S\delta/L_\epsilon$ of the porosity over a distance δ

$$0.212\left(\frac{\delta}{L_Y}\right)^{-\frac{1}{\nu}} \approx \frac{S\delta}{L_\epsilon}\cdot \tag{17}$$

This yields

$$\delta \approx \eta^{-\frac{1}{1+\nu}} L_\epsilon \tag{18}$$

where η is an heterogeneity index which combines the standard deviation S and the scale ratio L_ϵ/L_Y

$$\eta = \left(\frac{S}{0.212}\right)^{\nu} \frac{L_\epsilon}{L_Y}\cdot \tag{19}$$

If R is equated with L_Y and G with S/L_ϵ, within multiplicative constants, (16) yields

$$\sigma_x \propto L_\epsilon \eta^{-\frac{1}{1+\nu}} \tag{20}$$

in agreement with the prediction (18) for δ. Hence, our model is consistent with [33].

On the other hand, the volumetric area $\mathcal{A}$ of the surface where $\epsilon(\mathbf{r})$ equals $m_{\mathrm{c,h}}$ is inversely proportional to L_ϵ

$$\mathcal{A} = \frac{2\sqrt{2}}{L_\epsilon} \exp\left[-\frac{1}{2}\left(\frac{m_{\mathrm{c,h}}-E}{S}\right)^2\right] \tag{21}$$

as it follows from the formulae of Corrsin [34] (we introduced the factor 2 as a correction to a misprint). Hence, the volume fraction ϕ of the transition layer is

$$\phi(E) = \mathcal{A}\delta = \kappa \eta^{-\frac{1}{1+\nu}} \exp\left[-\frac{1}{2}\left(\frac{m_{\mathrm{c,h}}-E}{S}\right)^2\right]. \tag{22}$$

The constant κ is difficult to determine. It is of order 1 since the whole space is in the transition state if $\eta = 1$ and $E = m_{\mathrm{c,h}}$. In the following, it is set equal to $\sqrt{2}$, which provides a good agreement with the numerical data.

A sufficient condition to ensure global percolation is to increase E with respect to E_{c}^{∞} so that the region where ϵ is larger than $m_{\mathrm{c,h}}$ covers the whole transition zone, *i.e.*,

$$\frac{1}{\sqrt{2\pi}} \int_{\frac{m_{\mathrm{c,h}}-E}{S}}^{+\infty} \mathrm{e}^{-\epsilon^2/2} \mathrm{d}\epsilon \geq m_{\mathrm{c,h}} + \frac{\phi(E_{\mathrm{c}}^{\infty})}{2} \tag{23a}$$

or

$$E \geq E_{\mathrm{c}}(S,\eta) \qquad (L_\epsilon/L_Y \gg 1, \quad \eta \geq 1), \tag{23b}$$

with

$$E_{\mathrm{c}}(S,\eta) = m_{\mathrm{c,h}} + \sqrt{2}\, S\, \mathrm{erf}^{-1} \times \left\{2m_{\mathrm{c,h}} + \kappa\eta^{-\frac{1}{1+\nu}} \exp\left[-\frac{1}{2}\left(\frac{m_{\mathrm{c,h}}-E_{\mathrm{c}}^{\infty}}{S}\right)^2\right] - 1\right\}.$$

The former derivation is invalid if $\eta < 1$, since δ is then of the order of L_ϵ, and the medium cannot be regarded as a mixture of conducting and insulating regions separated by a transition layer. When η tends to infinity, the thickness δ becomes negligible with respect to L_ϵ, and accordingly, $E_{\mathrm{c}}(S,\eta)$ tends to $E_{\mathrm{c}}^{\infty}(S)$.

The critical porosity $m_{\mathrm{c}}(S,\eta)$ corresponding to $E_{\mathrm{c}}(S,\eta)$ is plotted in Figure 5 as a function of S and η.

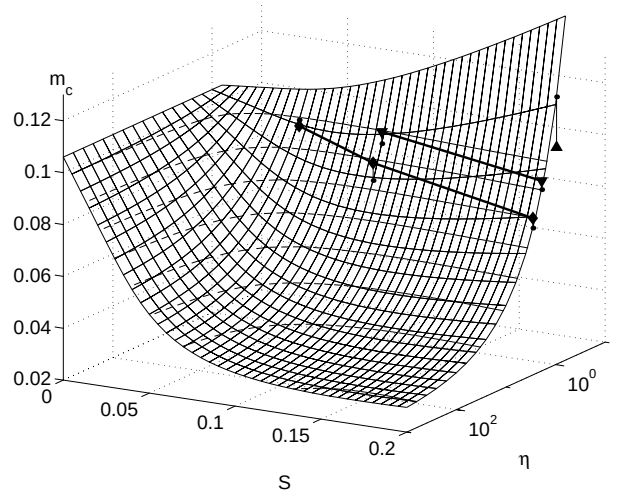

Fig. 5. Percolation threshold m_c corresponding to $E_c(S,\eta)$ in equation (23b), as a function of S and η, with $\kappa = \sqrt{2}$. The symbols are results of numerical simulations with $L_\epsilon/L_Y = 1$ (▲), 2 (▼) and 3 (⧫). The dots (•) are the projections of these data on the surface corresponding to the theoretical model.

For small η, the model is not applicable and equation (23) overestimates m_c. For $\eta \gg 1$, the convergence toward the limit m_c^∞ associated with E_c^∞ is very slow. For instance, with $S = 0.2$, m_c is about 0.08 for $\eta \approx 2.17$ ($L_\epsilon/L_Y = 3$), 0.05 for $\eta \approx 10$ ($L_\epsilon/L_Y \approx 14$), 0.04 for $\eta \approx 30$ ($L_\epsilon/L_Y \approx 40$) and becomes smaller than 0.03 for $\eta \geq 630$ ($L_\epsilon/L_Y \geq 870$). Hence, although a significant decrease of the percolation threshold is observed with the moderate ratios L_ϵ/L_Y, much stronger effects are expected with a sharper scale contrast.

3.3 Percolation in 2d

The argument leading to equations (15b) and (23b) can also be applied in two-dimensional media. However, the percolation threshold $m_{c,h}$ for 2d correlated media is equal to 1/2, and equations (15b, 23b) yields $E_c^\infty = E_c^\infty(S,\eta) = m_{c,h} = 1/2$ regardless of the values of S and η (or L_ϵ/L_Y).

Hence, in two-dimensions, these formulae predict that the position dependent threshold $\epsilon(\mathbf{r})$ does not affect the percolation threshold, which is a remarkable result. This was directly checked by numerical simulations on two-dimensional samples with $L/L_\epsilon = 20.48$, $L_Y/a = 10$ and two values of L_ϵ/L_Y. The percolation probability P has been calculated for various $\langle m\rangle$ and fixed S, and the average concentration m_a has been determined by using equation (11). The numerical results presented in Table 1 show that the variation of S does not influence m_a, and the fluctuations of the latter are within the limits of the statistical error interval.

Note that this lack of influence of heterogeneity in the 2d percolation problem is not limited to the Gaussian porosity fields considered here. Suppose that the statistical distribution of ϵ is characterized by the probability density $f_{E,S}$, and the distribution function $F_{E,S}$ is parameterized by its mean E and a measure S of its fluctuations. Equation (15) states that E_c^∞ corresponds to

Table 1. The averaged concentration m_a (*cf.* (11)) as a function of S for two-scale media in 2d for $L/L_\epsilon = 20.48$ and $L_Y/a = 10$. Data in parentheses are 95% confidence intervals.

L_ϵ/L_Y	m_a			
	$S=0$	0.1	0.2	0.3
2.5	0.503(0.003)	0.506(0.004)	0.503(0.005)	
5	0.506(0.002)	0.505(0.002)	0.505(0.002)	0.504(0.003)

$$F_{E_c^\infty,S}(m_{c,h}) = 1 - m_{c,h} \tag{24}$$

in two-dimensions, with $m_{c,h} = 1/2$, $E_c^\infty = 1/2$ for any porosity distribution for which the mean E and median M are equal.

More generally, equation (24) shows that the influence of heterogeneity on percolation depends on the statistical distribution of ϵ. For instance, if $f_{E,S}$ is given by

$$f_{E,S}(\epsilon) = \begin{cases} \frac{1-E}{E}(\beta+1)\left(\frac{E-\epsilon}{E}\right)^\beta, & 0 \leq \epsilon < E \\ \frac{E}{1-E}(\beta+1)\left(\frac{\epsilon-E}{1-E}\right)^\beta, & E \leq \epsilon \leq 1 \end{cases} \tag{25}$$

then $F_{E,S}(E) = 1 - E$ and $E_c^\infty = m_{c,h}$ in any dimensions. It is even possible to build distributions $f(\epsilon)$ that yield $E_c^\infty > m_{c,h}$.

Hence, in order to provide a counterexample, it is necessary to apply the previous argument to lognormally distributed porosities, for instance. Consider a lognormal probability density $f_{E,S}(\epsilon)$ with mean E and standard deviation S

$$f_{E,S}(\epsilon) = \frac{1}{\Sigma\epsilon\sqrt{2\pi}} \exp\left[-\frac{(\ln\epsilon - \ln\epsilon_0)^2}{2\Sigma^2}\right] \tag{26}$$

$$\epsilon_0 = E\left[1 + \left(\frac{S}{E}\right)^2\right]^{-1/2}, \quad \Sigma^2 = \ln\left[1 + \left(\frac{S}{E}\right)^2\right].$$

When equation (24) is applied for the lognormal distribution of ϵ, with $m_{c,h} = 1/2$ for two-dimensional percolation, it yields the critical value E_c^∞ in the form

$$E_c^\infty = \frac{1}{2}\sqrt{\frac{1}{2} + \sqrt{4S^2 + \frac{1}{4}}}\,. \tag{27}$$

Hence, E_c^∞ is larger than $m_{c,h}$ for any value of S. For instance, substituting $S = 0.15$ in equations (27) and (A.4) yields the critical porosity $m_c^\infty \approx 0.52$.

Without actually determining the precise value of m_c, it was checked numerically that the introduction of lognormal fluctuations of porosity decreases the percolation probability in two dimensions, for a given sample size L and mean porosity $\langle m\rangle$. Numerical tests performed for $\langle m\rangle = 0.5$ on samples with $L/L_\epsilon = 10.24$ and $L_\epsilon/L_Y = 2.5$

gave the percolation probabilities $P = 0.416(\pm 0.004)$ and $P = 0.40(\pm 0.01)$ for $S = 0$ and 0.15, respectively; for samples with $L/L_\epsilon = 20.48$ the corresponding values were $0.34(\pm 0.01)$ and $0.32(\pm 0.01)$, respectively. The difference in percolation probability is small and very large numbers of random realizations (6400 and 4000) had to be examined in order to sufficiently reduce the statistical error intervals. Nevertheless, the results support the prediction of the theoretical argument.

4 Numerical study in three dimensions

The present study is limited to media with Gaussian porosity distribution.

In order to check our methodology, the finite-size scaling method was first applied to one-scale porous media ($S = 0$). This study is reported in Appendix C and it can be summarized as follows. Discretization effects could be eliminated by extrapolating the results to the limit $L_Y/a \to \infty$. The critical porosity m_c is shown to be equal to 0.1063 (± 0.0007); the difference between this value and 0.3117 found for random uncorrelated site lattices is discussed; this value is also in excellent agreement with the one obtained by Mendelson [2]. The critical exponent ν is found to be equal to 0.79 (± 0.04) which is slightly smaller than the classical value $\nu = 0.88$ for the three-dimensional random lattices.

For two-scale porous media, the percolation threshold m_c and the exponent ν depend on two parameters, the ratio L_ϵ/L_Y and the variance S^2. First, the average concentration m_a and the width of the transition zone Δ_a were estimated for fixed a, L_Y, L_ϵ and L. Figure 6 shows a typical example of variation of m_a and Δ_a with the ratio a/L_Y for heterogeneous porous media. As in one-scale percolation (see Appendix C), the numerical data are well gathered by the scalings

$$m_a - m_a^* = r_1 \left(\frac{a}{L_Y}\right)^2 \tag{28a}$$

$$\Delta_a - \Delta_a^* = r_2 \left(\frac{a}{L_Y}\right). \tag{28b}$$

These scalings provide the asymptotic values m_a^* and Δ_a^* which still depend upon L_ϵ/L_Y, S and L/L_ϵ.

Thus, we still need to extrapolate to an infinite value of the ratio L/L_ϵ. This can be done by using the scaling laws (14), which contain two unknown coefficients, namely ν and m_c. The most obvious procedure consists of deriving ν from (14b), then to deduce m_c from (14a), by using this value of ν.

This procedure is illustrated in Figure 7 and its results are gathered in Table 2 that we shall present briefly. The regression lines of Δ_a^* as functions of L/L_ϵ yield values ν_1 for ν which are slightly different for each pair of parameters S and L_ϵ/L_Y. The regression coefficients are always larger than 0.985.

These values of ν_1 are used to represent m_a^* as a function of $(L/L_\epsilon)^{-\nu_1}$ according to (14a) and to obtain the percolation threshold m_c. This step is illustrated in Figure 7b. It is worth noting that the correlation coefficients are larger than 0.997; the statistical fit is thus excellent.

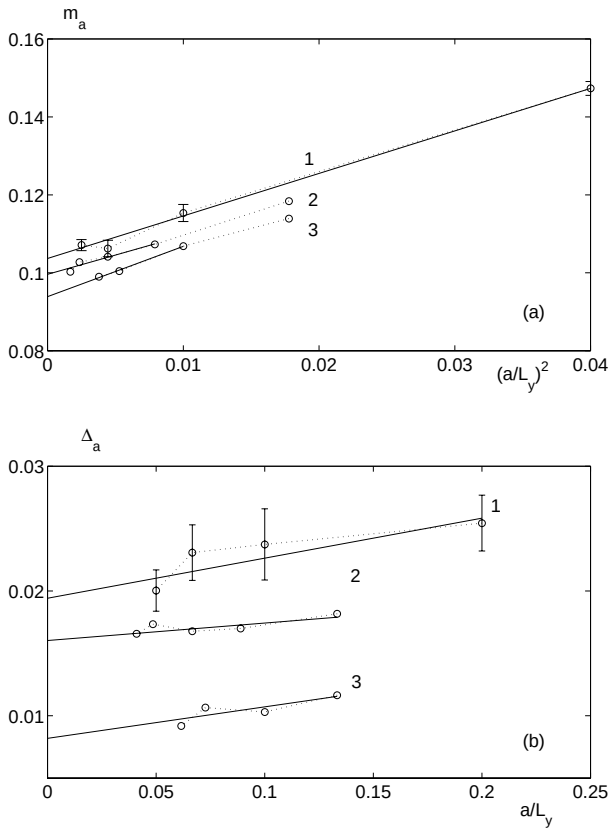

Fig. 6. The average concentration m_a (a) and the width of transition zone Δ_a (b) as functions of a/L_Y for two-scale porous media with $S = 0.1$ and $L_\epsilon/L_Y = 3$. Data are for $L/L_\epsilon = 2.13$ (1), 2.84 (2) and 4.27 (3). Solid lines represent linear fits. Vertical bars give statistical error intervals for the numerical data, obtained for 3 percolation tests on 20 to 30 random realizations.

As a check, equation (14a) can be used a second time in order to estimate the overall statistical precision. Here, m_c is known and another value ν_2 is obtained through a second fit of $m_a^* - m_c$ as a function of L/L_ϵ. This is illustrated in Figure 7c; the regression coefficients are always larger than 0.992. Moreover, it is seen in Table 2 that the two estimations of ν never differ by more than 2.2%, except for ($S = 0.2$, $L_\epsilon/L_Y = 3$), where the discrepancy reaches 4%. Hence, this can be considered as a successful test for the whole procedure of the finite-size scaling method. Note that other consistency checks were performed which are not reported here; for instance, the scaling (14) was performed on E instead of m, and m_c deduced from E_c by equation (A.3); no significant difference was found (see Tab. 2).

For $L_\epsilon/L_Y = 1$, the percolation threshold does not differ much from the value 0.1063 obtained for one-scale porous media. With increasing L_ϵ/L_Y, m_c decreases, and for $L_\epsilon/L_Y = 3$, $S = 0.2$, it reaches the value $0.0809(\pm 0.0012)$. Unfortunately, the computers with

Table 2. The critical exponent ν and the percolation thresholds m_c and E_c as functions of the ratio L_ϵ/L_Y and S for homogeneous and heterogeneous media. m_c was directly evaluated by the finite size technique (14) applied to m, deduced from E_c through (A.3), estimated from (23b).

	$S=0$	$S=0.05$	$S=0.1$			$S=0.2$		
		$\frac{L_\epsilon}{L_Y}=3$	$\frac{L_\epsilon}{L_Y}=1$	$\frac{L_\epsilon}{L_Y}=2$	$\frac{L_\epsilon}{L_Y}=3$	$\frac{L_\epsilon}{L_Y}=1$	$\frac{L_\epsilon}{L_Y}=2$	$\frac{L_\epsilon}{L_Y}=3$
ν_1	0.79	0.90	0.70	0.70	0.93	0.86	0.76	0.69
ν_2	0.82	0.89	0.70	0.71	0.90	0.86	0.77	0.72
m_c (14)	0.1063	0.0968	0.1078	0.1001	0.0861	0.1036	0.0933	0.0804
m_c (A.3)	0.1063	0.0977	0.1080	0.1005	0.0876	0.1039	0.0940	0.0809
m_c (23b)				0.0955	0.0899	0.0990	0.0828	0.0766
E_c	0.1063	0.0972	0.0996	0.0906	0.0743	0.0444	0.0269	0.0022

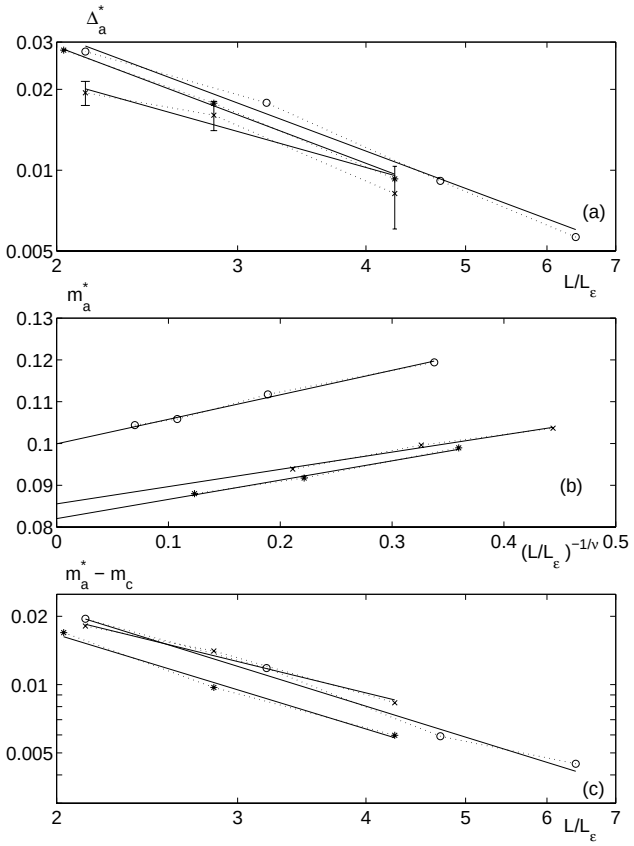

Fig. 7. Log-log plots of Δ_a^* as a function of L/L_ϵ (a), of m_a^* as a function of $(L/L_\epsilon)^{-1/\nu}$ (b) and of $m_a^* - m_c$ as a function of L/L_ϵ (c) for two-scale porous media with $S=0.1, L_\epsilon/L_Y=2$ ($\circ$); $S=0.1, L_\epsilon/L_Y=3$ ($\times$) and $S=0.2, L_\epsilon/L_Y=3$ ($*$). Solid lines represent linear fits, and vertical bars show statistical error intervals.

512 Mbytes memory used in this numerical study have not permitted to go farther than 3 in the analysis of the influence of L_ϵ/L_Y on the percolation threshold, and a theoretical approach has been developed, which was discussed in Section 3. The critical porosity m_c obtained numerically is plotted in Figure 5 as a function of S and η, in comparison with the theoretical data. The constant κ was set to $\sqrt{2}$, which yields a very good concordance between the theoretical model and the numerical data for $\eta \geq 0.8$. For smaller η, the model is not applicable and equation (23) overestimates m_c, as illustrated by the numerical results for ($S=0.20$, $L_\epsilon/L_Y=1$) or ($S=0.05$, $L_\epsilon/L_Y=3$) which both correspond to $\eta=0.72$ (see Tab. 2).

In summary, the present study shows that the percolation threshold for three-dimensional two-scale porous media with a Gaussian porosity field is smaller than that for one-scale media, which is a very important result. It decreases with increasing porosity variation amplitude S (at least for S smaller than or comparable to $m_{c,h}$), and with increasing contrast between the typical pore size and heterogeneity scale, quantified by the ratio L_ϵ/L_Y.

The critical exponent ν is found to vary slightly with S and L_ϵ/L_Y (see Tab. 2). There is no clear systematic deviation from the value for the one-scale case, which would be larger than the error interval.

These findings agree with results of Weinrib [4] and Schmittbuhl *et al.* [5] who concluded that critical exponents are insensitive to the presence of short-range correlations, such as (3) and (5).

5 Conclusions

The percolation properties of two-scale porous media generated by nonlinear filtering of Gaussian random correlated field with a random Gaussian spatially correlated threshold field have been numerically analyzed. The percolation threshold and the critical exponent ν were derived with the help of a finite-size scaling method. The percolation threshold is a decreasing function of the porosity field variance S^2, and of the ratio of correlation lengths, L_ϵ/L_Y. Their combined influence can be described by the heterogeneity η. Neither the correlation lengths nor the variance S^2 significantly influence the critical exponents with a clear change of universality class relative to the case of uncorrelated lattices.

A theoretical argument can be proposed for the estimation of the percolation threshold in the two-scale media, when the percolation on the two scales can be analyzed separately by using results for one-scale porous media.

It is shown that different effects can be observed in 2 and 3 dimensions, and that the sign and amplitude of the threshold variation depend on the porosity probability distribution. In particular, lognormally distributed porosity fluctuations yield percolation thresholds lower and higher in two and three dimensions, respectively, than uniform porosity.

This last character is particularly important for real media since porosity often obeys a lognormal distribution. This work will be extended to this situation in the near future.

Most computations were performed at CINES (subsidized by the MENESR) whose support is gratefully acknowledged. This work has been partly supported by the EU Thermie Project OG/263/98/HE/NO/FR.

Appendix A: Mean porosity of a two-scale porous medium

The statistical mean $\langle m\rangle$ of the porosity of a two-scale porous medium under consideration does not depend upon L_Y and L_ϵ, and can be derived from the definition (7)

$$\langle m\rangle = \langle Z\rangle = \int_{-\infty}^{\infty} \mathrm{d}y \int_{-\infty}^{p(y)} \mathrm{d}\epsilon f(\epsilon)\psi_1(y), \tag{A.1}$$

where

$$f(\epsilon) = \frac{1}{\sqrt{2\pi}S}\exp\left(-\frac{(\epsilon-E)^2}{2S^2}\right), \tag{A.2a}$$

$$\psi_1(y) = \frac{\mathrm{d}p}{\mathrm{d}y} = \frac{1}{\sqrt{2\pi}}\exp\left(-\frac{y^2}{2}\right). \tag{A.2b}$$

Substitution of $f(\epsilon)$ and $\psi_1(y)$ into the right-hand side of equation (A.1) yields

$$\langle m\rangle = \frac{S}{\sqrt{2\pi}}\left\{\exp\left(-\frac{E^2}{2S^2}\right) - \exp\left(-\frac{(1-E)^2}{2S^2}\right)\right\} + \frac{1-E}{2}\mathrm{erfc}\left(\frac{1-E}{\sqrt{2}S}\right) + \frac{E}{2}\mathrm{erfc}\left(-\frac{E}{\sqrt{2}S}\right). \tag{A.3}$$

Figure 2 shows $\langle m\rangle$ as functions from E and S. It can be seen that the mean porosity $\langle m\rangle$ is generally different of E, except for $S = 0$, as already stated. $\langle m\rangle$ is an increasing function of S for $E < 0.5$ and a decreasing one for $E > 0.5$. Note that the mean porosity $\langle m\rangle$ is a regular increasing function of E ranging between 0 and 1.

For $E = 0.5$, $\langle m\rangle$ is equal to 0.5 for all S. When S tends to infinity, the mean porosity tends to 0.5. It can be seen that equation (A.3) is invariant under the transformation $\langle m\rangle \to 1 - \langle m\rangle$ and $E \to 1 - E$, which is a simple consequence of the symmetry of the definition (4) of the phase function Z relative to liquid and solid phases.

The mean porosity $\langle m\rangle$ of a two-scale medium described by a lognormal probability distribution (26) can be derived similarly and expressed as

$$\langle m\rangle = \frac{E}{2}\mathrm{erfc}\left(\frac{\ln\epsilon_0 + \Sigma^2}{\sqrt{2}\Sigma}\right) + \frac{1}{2}\mathrm{erfc}\left(-\frac{\ln\epsilon_0}{\sqrt{2}\Sigma}\right). \tag{A.4}$$

Appendix B: Covariance of the phase function in two-scale media

The spatial statistical properties of the phase function $Z(\mathbf{r})$ are described by the covariance function

$$C_Z(\mathbf{r},\mathbf{s}) = \langle [Z(\mathbf{r}) - \langle Z\rangle][Z(\mathbf{s}) - \langle Z\rangle]\rangle. \tag{B.1}$$

When the random fields Y and ϵ are homogeneous and isotropic in the statistical sense, the phase function Z is also a homogeneous isotropic random field, whose covariance C_Z only depends upon the distance $r = \|\mathbf{r}-\mathbf{s}\|$. The covariance C_Z can be expressed for a given r similarly to $\langle Z\rangle$ (*cf.* (A.1)) as

$$C_Z = \int_{-\infty}^{\infty}\mathrm{d}y_1\int_{-\infty}^{\infty}\mathrm{d}y_2\psi_2(y_1,y_2)\int_{-\infty}^{p(y_1)}\mathrm{d}\epsilon_1 \times \int_{-\infty}^{p(y_2)}\mathrm{d}\epsilon_2 f_2(\epsilon_1,\epsilon_2) - \langle Z\rangle^2, \tag{B.2a}$$

$$f_2(\epsilon_1,\epsilon_2) = \frac{1}{2\pi S^2\sqrt{1-(\frac{C_\epsilon}{S^2})^2}}\exp\left[-\frac{t_1^2 - 2C_\epsilon t_1 t_2/S^2 + t_2^2}{2S^2(1-(\frac{C_\epsilon}{S^2})^2)}\right], \quad t_i = \epsilon_i - E, \tag{B.2b}$$

$$\psi_2(y_1,y_2) = \frac{1}{2\pi\sqrt{1-C_Y^2}}\exp\left[-\frac{y_1^2 - 2C_Y y_1 y_2 + y_2^2}{2(1-C_Y^2)}\right], \tag{B.2c}$$

where the values y_i and ϵ_i ($i = 1, 2$) are evaluated at the points $\mathbf{r}$ and $\mathbf{s}$ separated by a distance r.

For one-scale porous media ($S = 0$), the number of integrations in (B.2a) can be reduced to 1 (see [11]), and the covariance of the phase function can be written as

$$C_Z = \int_0^{C_Y}\frac{\mathrm{d}t}{2\pi\sqrt{1-t^2}}\exp\left(-\frac{y_m^2}{1+t}\right), \quad p(y_m) = E. \tag{B.3}$$

Figure 3 shows a typical normalized covariance C_Z/σ_Z^2, $\sigma_Z^2 = C_Z(r = 0)$ in comparison with the corresponding covariance C_Y. The prediction of equation (B.3) and the covariance of the phase function Z, numerically calculated as the spatial average instead of the statistical one in equation (B.1) for a single statistical realization of a porous media, are in good agreement.

The influence of S and of L_Y/L_ϵ on C_Z for two-scale porous media is illustrated in Figure 3. It appears that identical C_Z/σ_Z^2 are obtained for one- media and two-scale media if $L_\epsilon = L_Y$, whereas C_Z increases for $L_\epsilon > L_Y$. The range and amplitude of this increment are increasing functions of L_ϵ and S, respectively.

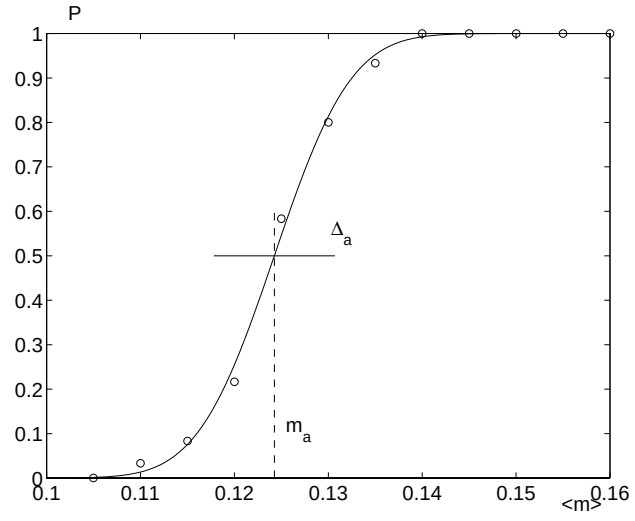

Fig. 8. Percolation probability P *vs.* $\langle m \rangle$ for one-scale porous media ($S = 0$). Data are for $L/L_Y = 12.8$ and $L_Y/a = 10$. Circles represent the numerical data, obtained by performing $N = 30$ percolation tests; the solid line corresponds to the best fit given by equation (11). The horizontal bar shows Δ_a and the dashed vertical bar the position of m_a.

Appendix C: Percolation in two-scale porous media

The finite-size scaling technique discussed in Section 2.2 was first applied to homogeneous porous media, as a check for the methodology.

C.1 Discretization effects

In order to analyze and subsequently eliminate the influence of discretization, the percolation probability P has been calculated as a function of $\langle m \rangle$ for fixed values of the ratio L/L_Y and an increasing resolution L_Y/a. In Figure 8, $P(\langle m \rangle)$ is displayed for $L_Y/a = 10$. When the resolution increases, the interval where P rises from 0 to 1 is shifted towards 0, and m_a asymptotically reaches m_a^* when $L_Y/a \to 0$.

It was found that $m_a(L_Y/a)$ is well represented by linear functions of $(L_Y/a)^{-2}$; with correlation coefficients greater than 0.99. By extrapolating these linear fits, asymptotic values m_a^* are determined in the limit $a/L_Y = 0$ for various ratios L/L_Y. This dependency is summarized by the formula (28a).

Various representations of Δ_a against $(L_Y/a)^{-b}$ with $0.5 < b < 2$ were tried. For all b, the χ^2- measure was calculated, but no b gave a clear minimum. Fortunately, it was found that the value of b has little influence on the percolating threshold and the exponent ν; thus, $b = 1$ has been chosen for subsequent extrapolation of Δ_a in the limit $a/L_Y = 0$ (see (28b)).

C.2 Percolation threshold and exponent ν

According to equation (14b) a log-log plot of Δ_a^* *vs.* L/L_Y has been used to determine ν. A linear fit of the numerical data gave a value of $\nu = 0.79(\pm 0.04)$, which is slightly smaller than the classical one $\nu = 0.88$ for the three-dimensional site percolation problem on random lattices [1]. The correlation coefficient r of the statistical regression is equal to 0.997; hence, the statistical precision is good.

The averaged concentration m_a^* plotted against $(L/L_Y)^{-1/\nu}$ follows the scaling law (14a) very closely, with a correlation coefficient $r = 0.9985$, and m_a^* tends to the limit $m_{c,h} = 0.1063(\pm 0.0007)$, where the subscript h refers to homogeneous media.

This value differs substantially from 0.3117 found for random uncorrelated sites lattices [1]. Although it has often been demonstrated that spatial correlations significantly lower the percolation threshold with respect to uncorrelated lattice percolation (see *e.g.*, [3,4,13,35–39]), only the results of [2] can be directly compared with the present data; all other studies were restricted to two-dimensional media or considered other types of correlations with longer ranges such as negative exponentials or power laws. Mendelson [2] considered correlated media built in the following way. A continuous field Y was obtained by the convolution of a random uncorrelated field, uniformly distributed between 0 and 1, with a smoothing function K. Our value of $m_{c,h}$ is in perfect agreement with the extrapolation for $L \to \infty$ by Mendelson [2] of the threshold for a Gaussian smoothing function K, which yielded $m_c = 0.106$. The latter agrees well with the value $m_{c,h} = 0.1063$ determined in the present study. Roberts and Teubner [11] and Ioannidis *et al.* [13] reported the values 0.13 and 0.09, respectively, for the percolation threshold on lattices which were generated by using other forms of the covariance C_Y than Gaussian, but which also corresponded to statistically continuous random fields Y.

For comparison, numerical results for uncorrelated site percolation were analyzed for L ranging from 16 to 256. The percolation threshold was found to be equal to $m_{c,u} = 0.31151$ (± 0.00006), with $\nu = 0.88(\pm 0.02)$, in very good agreement with the accepted values, 0.3117 and 0.88, respectively.

The dependencies of m_a and Δ_a upon L/L_Y and L_Y/a for homogeneous media can be summarized by

$$m_a = m_{c,h} + 1.314 \left(\frac{a}{L_Y}\right)^2 + 0.1068 \left(\frac{L}{L_Y}\right)^{-1/\nu} \quad \text{(C.1a)}$$

$$\Delta_a = \left[0.129 \left(\frac{a}{L_Y}\right) + 0.212\right] \left(\frac{L}{L_Y}\right)^{-1/\nu}. \quad \text{(C.1b)}$$

The scaling behavior of the percolating cluster which is characterized by the critical exponent ν seems to be similar for both correlated and uncorrelated cases when the covariance function (3) is used for the generation of the porous media. The little difference in values of ν found for these cases does not clearly indicate that they belong to different universality classes, because of the low precision of the determination of ν.

References

1. D. Stauffer, A. Aharony, *Introduction to Percolation Theory*, 2nd edn. (Taylor and Francis, Bristol, 1994).
2. K.S. Mendelson, Phys. Rev. E **56**, 6586 (1997).
3. V.V. Mourzenko, J.-F. Thovert, P.M. Adler, Phys. Rev. E **53**, 5606 (1996).
4. A. Weinrib, Phys. Rev. B **29**, 387 (1984).
5. J. Schmittbuhl, J.-P. Vilotte, S. Roux, Phys. Rev. A **26**, 6115 (1993).
6. M. Sahimi, S. Mukhopadhyay, Phys. Rev. E **54**, 3870 (1996).
7. J.W. Cahn, J. Chem. Phys. **42**, 93 (1965).
8. M.Y. Joshi, Ph.D. thesis, University of Kansas, Lawrence, KS, 1974.
9. J.A. Quiblier, J. Coll. Intefr. Sci. **98**, 84 (1984).
10. P.M. Adler, *Porous Media: Geometry and Transports* (Butterworth/Heinemann, Stoneham, MA, 1992).
11. A.P. Roberts, M. Teubner, Phys. Rev. E **51**, 4141 (1995).
12. A.P. Roberts, M.A. Knackstedt, Phys. Rev. E **54**, 2313 (1996).
13. M.A. Ioannidis, M.J. Kwiecien, I. Chatzis, Transp. Porous Media **29**, 61 (1997).
14. C.L.Y. Yeong, S. Torquato, Phys. Rev. E **57**, 495 (1998).
15. C.L.Y. Yeong, S. Torquato, Phys. Rev. E **58**, 224 (1998).
16. E.J. Garboczi, D.P. Bentz, in *Annual Review of Computational Physics*, edited by D. Stauffer (World Scientific, Singapore, 1999).
17. P.M. Adler, J.-F. Thovert, Appl. Mech. Rev. **51**, 537 (1998).
18. R. Hilfer, Phys. Rev. B **44**, 60 (1991).
19. R. Hilfer, Phys. Rev. B **45**, 7115 (1992).
20. R. Hilfer, in *Advances in Chemical Physics*, Vol. 92, edited by I. Prigogine, S.A. Rice (Wiley, New York, 1996).
21. C.P. Fernandes *et al.*, Transp. Porous Media **20**, 3 (1996).
22. A.V. Neimark, Sov. Phys. JETP **69**, 786 (1989).
23. M. Sahimi, *Flow and transport in porous media and fractured rock* (VCH, Weinheim, 1995).
24. R.D. Hazlett, Math. Geology **29**, 801 (1997).
25. A. Adrover, M. Giona, Ind. Eng. Chem. Process **36**, 5010 (1997).
26. N.F. Berk, Phys. Rev. Lett. **58**, 2718 (1987).
27. A.P. Roberts, Phys. Rev. E **55**, R1286 (1997).
28. A.P. Roberts, Phys. Rev. E **56**, 3203 (1997).
29. P.M. Adler, C.J. Jacquin, J.A. Quiblier, Int. J. Multiph. Flow **16**, 691 (1990).
30. J.-F. Thovert, J. Salles, P.M. Adler, J. Microscopy **170**, 65 (1993).
31. P.J. Reynolds, H.E. Stanley, W. Klein, Phys. Rev. B **21**, 1223 (1980).
32. M. Rosso, J.F. Gouyet, B. Sapoval, Phys. Rev. Lett. **57**, 3195 (1986).
33. J. Quintanilla, S. Torquato, J. Chem. Phys. **111**, 5947 (1999).
34. S. Corrsin, Quart. Appl. Math. **12**, 404 (1954).
35. A. Weinrib, Phys. Rev. B **26**, 1352 (1982).
36. S. Prakash *et al*, Phys. Rev. A **46**, 1724 (1992).
37. D.A. Wollman, M.A. Dubson, Q. Zhu, Phys. Rev. B **48**, 3713 (1993).
38. M. Sahimi, J. Phys. I France **4**, 1263 (1994).
39. R.E. Amritkar, M. Roy, Phys. Rev. E **57**, 1269 (1998).